Path-integrals and the BEC/BCS crossover in dilute atomic gases

J. Tempere

TFVS, Universiteit Antwerpen, Universiteitsplein 1, B2610 Antwerpen, Belgium.

J.T. Devreese

TFVS, Universiteit Antwerpen, Universiteitsplein 1, B2610 Antwerpen, Belgium.

Both the trapping geometry and the interatomic interaction strength of a dilute ultracold fermionic gas can be well controlled experimentally. When the interactions are tuned to strong attraction, Cooper pairing of neutral atoms takes place and a BCS superfluid is created. Alternatively, the presence of Feshbach resonances in the interatomic scattering allow populating a molecular (bound) state. These molecules are more tightly bound than the Cooper pairs and can form a Bose–Einstein condensate (BEC). In this contribution, we describe both the BCS and BEC regimes, and the crossover, from a functional integral point of view. The path-integral description allows to derive the properties of the superfluid (such as vortices and Josephson tunneling) and follow them as the system is tuned from BCS the BEC.

PACS: 03.75.-b, 03.75.Lm
Key words: superfluidity, BEC/BCS crossover

1 The ultracold dilute Fermi gas

When a dilute Bose gas is cooled below the degeneracy temperature, the bosonic atoms all condense in the same one-particle state and a Bose–Einstein condensate forms. This has been convincingly demonstrated with magnetically trapped, evaporatively cooled atomic gases for a multitude of atom species. Moreover, magnetic or optical traps can be equally well loaded with fermionic isotopes, such as ^{6}Li or ^{40}K. These atoms do not undergo Bose–Einstein condensation, but fill up a Fermi sea, as has been demonstrated through the observation of the Pauli blocking effect [1] and through a measurement of the total energy of the Fermi gas [2]. Very soon after the observation of a degenerate Fermi sea of atoms, researchers embarked upon the quest to achieve Cooper pairing in the dilute Fermi gas. Indeed, for metals we know that the Fermi sea is unstable with respect to Cooper pair formation. So, if the (neutral) atoms in the dilute gas attract each other, a similar instability towards a paired state is to be expected.

The interatomic interactions in ultracold gases are remarkable for two reasons. Firstly, the collisions between the atoms can be satisfactorily characterized by a single number, the s-wave scattering length a_s. For low-energy collisions, the effective interaction potential between atoms becomes a contact potential, $V(\mathbf{r}-\mathbf{r}') = g\delta(\mathbf{r}-\mathbf{r}')$, where $g = 4\pi\hbar a_s/m$ with m the mass of the atoms. The scattering length can be both positive (leading to interatomic repulsion) or negative (attraction).

Secondly, this scattering length can be tuned by an external magnetic field when a Feshbach resonance is present [3]. This resonance occurs when the energy of a bound (molecular) state in a closed scattering channel becomes equal to the energy of the colliding atoms in the open scattering channel. The different channels correspond here to different hyperfine states of the trapped atoms, and the distance in energy between these states can be tuned with a magnetic field.

In what follows, we will consider a trapped mixture of ^{40}K atoms in the $\left|\frac{9}{2},-\frac{7}{2}\right\rangle$ and $\left|\frac{9}{2},-\frac{9}{2}\right\rangle$ hyperfine states. This potassium isotope is fermionic, and the trapped states display a Feshbach resonance at $B = 202.1$ Gauss. When the scattering length is tuned to a negative value, the atoms attract and Cooper pairs can form leading to a *BCS regime*. The critical temperature for Cooper pairing can be raised by making the scattering length more strongly negative. When the scattering length is large and positive, the molecular state in the closed channel is populated, and molecules appear that can be Bose–Einstein condensed (the *BEC regime*). The adaptability of the scattering length allows bringing the gas from the BCS regime into the BEC regime or vice versa, and allows studying the interesting intermediate 'crossover' regime.

The first experimental realization of superfluidity of a Fermi gas in the molecular BEC regime came in 2003 [4]. A condensate of molecules was convincingly observed. The detection of superfluidity in the BCS regime however is much more subtle. In an initial experiment [5], the superfluid behavior was derived from the hydrodynamic nature of the expansion of the cloud, as compared to a ballistic expansion expected for a non-superfluid weakly-interacting Fermi gas [6]. However, this did not constitute unambiguous proof, since the Fermi gas was in the strongly interacting regime. Subsequent experiments probed superfluidity by mapping the pair density onto a molecular condensate density [7] or by spectroscopically measuring the gap [8]. Yet although these experimental methods clearly demonstrate pairing, they do not unambiguously demonstrate superfluid behavior.

The very recent observation of a lattice of quantized vortices in resonant Fermi gases [9] constitutes the first clear demonstration of superfluidity in the BEC/BCS regime. Observation of these vortices well in the BCS regime may be difficult since the fermionic density penetrates in the core of the vortex in the BCS regime, leading to a loss of contrast in direct imaging [10, 11, 9]. Another possibility to demonstrate superconductivity is though the observation of the Josephson effect [12] in optical lattices. These optical lattices are periodic potentials formed by two counterpropagating laser beams, for example in the z-direction:

$$V_{\rm opt}(z) = sE_R \sin^2(2\pi z/\lambda)\,, \tag{1}$$

where λ is the laser wave length, $E_R = h^2/(2m\lambda^2)$ is the recoil energy, and s is the laser intensity expressed in units of the recoil energy. Typically, $s = 1-20$, $\lambda = 795$ nm. The atoms collect in the valleys of the optical lattice and form a "stack of pancakes", illustrated in Fig. 1. Typically, there are on the order of a few 100 'pancakes' with on the order of 1000 atoms each. When a superfluid is loaded in such an optical lattice, the system corresponds to an array of Josephson junctions.

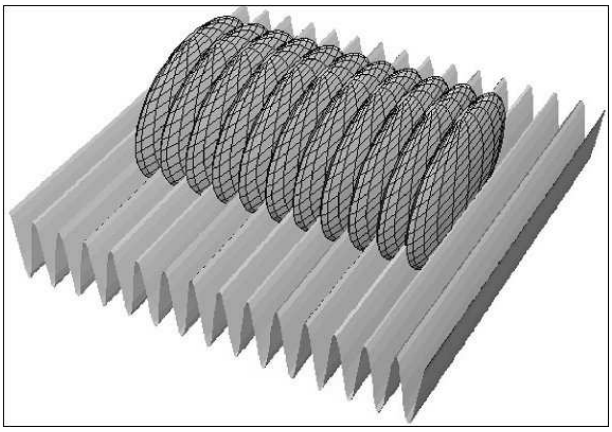

Fig. 1. Two counterpropagating laser beams form a periodic potential for the atoms. Such optical lattices can be loaded with quantum gases, forming a stack of quasi-two dimensional clouds.

In such an array, the superfluid gas can propagate whereas the normal state gas is pinned. This has already been demonstrated for bosonic atoms [13], and has been predicted theoretically for fermionic atoms [12, 14].

2 Path-integral treatment of the BEC/BCS crossover

The partition function for the atomic Fermi gas is given by the functional integral

$$\mathcal{Z} = \int \mathcal{D}\bar{\psi}_{\mathbf{x},\tau,\sigma}\mathcal{D}\psi_{\mathbf{x},\tau,\sigma}\exp\left\{-\mathcal{S}/\hbar\right\} \tag{2}$$

with an action

$$\begin{aligned}\mathcal{S} = &\int_0^{\hbar\beta} \mathrm{d}\tau \int \mathrm{d}\mathbf{x} \sum_\sigma \bar{\psi}_{\mathbf{x},\tau,\sigma}\left(\hbar\,\frac{\partial}{\partial\tau} - \frac{\hbar^2}{2m}\,\nabla_{\mathbf{x}}^2 - \mu\right)\psi_{\mathbf{x},\tau,\sigma} + \\ &+ \int_0^{\hbar\beta} \mathrm{d}\tau \int \mathrm{d}\mathbf{x}\, g\bar{\psi}_{\mathbf{x},\tau,\uparrow}\bar{\psi}_{\mathbf{x},\tau,\downarrow}\psi_{\mathbf{x},\tau,\downarrow}\psi_{\mathbf{x},\tau,\uparrow}\,.\end{aligned} \tag{3}$$

The fermionic fields $\psi_{\mathbf{x},\tau}, \bar{\psi}_{\mathbf{x},\tau}$ are Grassman variables. The interaction potential, as discussed in the previous section, is a contact potential with experimentally adjustable strength g. The two hyperfine states are denoted by $\sigma = \uparrow, \downarrow$. The functional integral over the Grassman variables can be performed analytically only for an action that is quadratic in $\psi_{\mathbf{x},\tau}, \bar{\psi}_{\mathbf{x},\tau}$. In order to get rid of the quartic term in (3) we perform a Hubbard–Stratonovic (HS) transformation, introducing auxiliary bosonic fields $\bar{\Delta}_{\mathbf{x},\tau}$ and $\Delta_{\mathbf{x},\tau}$:

$$\mathcal{Z} \propto \int \mathcal{D}\bar{\psi}_{\mathbf{x},\tau,\sigma}\mathcal{D}\psi_{\mathbf{x},\tau,\sigma}\int \mathcal{D}\bar{\Delta}_{\mathbf{x},\tau}\mathcal{D}\Delta_{\mathbf{x},\tau}\exp\left\{-\mathcal{S}/\hbar\right\} \tag{4}$$

with

$$\mathcal{S} = \int_0^{\hbar\beta} \mathrm{d}\tau \int \mathrm{d}\mathbf{x} \sum_\sigma \bar{\psi}_{\mathbf{x},\tau,\sigma} \left(\hbar \frac{\partial}{\partial \tau} - \frac{\hbar^2}{2m} \nabla_{\mathbf{x}}^2 - \mu \right) \psi_{\mathbf{x},\tau,\sigma} - \\ - \int_0^{\hbar\beta} \mathrm{d}\tau \int \mathrm{d}\mathbf{x} \left(\bar{\Delta}_{\mathbf{x},\tau} \psi_{\mathbf{x},\tau,\downarrow} \psi_{\mathbf{x},\tau,\uparrow} + \Delta_{\mathbf{x},\tau} \bar{\psi}_{\mathbf{x},\tau,\uparrow} \bar{\psi}_{\mathbf{x},\tau,\downarrow} + \frac{\bar{\Delta}_{\mathbf{x},\tau} \Delta_{\mathbf{x},\tau}}{g} \right). \tag{5}$$

Indeed, performing the functional integral over the HS fields $\bar{\Delta}_{\mathbf{x},\tau}$, $\Delta_{\mathbf{x},\tau}$ in (5) brings us back to (3). Our goal is an investigation of the superfluid properties of the ultracold Fermi system. For a straightforward hydrodynamic interpretation of the Hubbard–Stratonovic fields, it is advantageous to work with $|\Delta_{\mathbf{x},\tau}|$ and $\theta_{\mathbf{x},\tau}$. These are related to the original HS field by $\Delta_{\mathbf{x},\tau} = |\Delta_{\mathbf{x},\tau}| \exp(\mathrm{i}\theta_{\mathbf{x},\tau})$. We have restricted the functional integral to $\bar{\Delta}_{\mathbf{x},\tau} = (\Delta_{\mathbf{x},\tau})^*$ without neglecting any field configurations of importance to the final result. The hydrodynamic interpretation of $|\Delta_{\mathbf{x},\tau}|^2$ is the density of fermion pairs, whereas $\hbar \nabla_{\mathbf{x}} \theta_{\mathbf{x},\tau}/m = \mathbf{v}_{\mathbf{x},\tau}$ can be interpreted as the superfluid velocity field. Performing this change of variables in the functional integral yields

$$\mathcal{Z} \propto \int \mathcal{D}\bar{\psi}_{\mathbf{x},\tau,\sigma} \mathcal{D}\psi_{\mathbf{x},\tau,\sigma} \int \mathcal{D} |\Delta_{\mathbf{x},\tau}| \, \mathcal{D}\theta_{\mathbf{x},\tau} \exp\left\{ -\mathcal{S}/\hbar \right\}, \tag{6}$$

with

$$\mathcal{S} = \int_0^{\hbar\beta} \mathrm{d}\tau \int \mathrm{d}\mathbf{x} \bar{\psi}_{\mathbf{x},\tau,\sigma} \Bigg(\hbar \frac{\partial}{\partial \tau} - \frac{\hbar^2}{2m} \nabla_{\mathbf{x}}^2 - \frac{1}{2} \mathbf{v}_{\mathbf{x},\tau} \cdot \mathrm{i}\hbar \nabla_{\mathbf{x}} - \mu + \\ + \frac{\mathrm{i}\hbar}{2} \frac{\partial \theta_{\mathbf{x},\tau}}{\partial \tau} - \frac{1}{4} (\mathrm{i}\hbar \nabla_{\mathbf{x}} \cdot \mathbf{v}_{\mathbf{x},\tau}) + \frac{1}{8} m \mathbf{v}_{\mathbf{x},\tau}^2 \Bigg) \psi_{\mathbf{x},\tau,\sigma} - \\ - \int_0^{\hbar\beta} \mathrm{d}\tau \int \mathrm{d}\mathbf{x} \left(|\Delta_{\mathbf{x},\tau}| \, \psi_{\mathbf{x},\tau,\downarrow} \psi_{\mathbf{x},\tau,\uparrow} + |\Delta_{\mathbf{x},\tau}| \, \bar{\psi}_{\mathbf{x},\tau,\uparrow} \bar{\psi}_{\mathbf{x},\tau,\downarrow} + \frac{|\Delta_{\mathbf{x},\tau}|^2}{g} \right). \tag{7}$$

De Palo et al. [17] suggest at this point to introduce additional collective quantum variables to extract the fermionic density. However, care must be taken, since when additional collective quantum fields are present the problem of double-counting poses itself [18], and variational perturbation theory has to be applied to avoid double-counting [19]. However, in the present case it is not necessary to explicitly introduce the additional collective variables to obtain information about the atomic density profile [20]. In (6) the integration over the fermionic variables can be taken, leading to

$$\mathcal{Z} \propto \int \mathcal{D} |\Delta_{\mathbf{x},\tau}| \, \mathcal{D}\theta_{\mathbf{x},\tau} \exp\left\{ -\mathcal{S}_{\mathrm{eff}}/\hbar \right\} \tag{8}$$

with an effective action

$$\mathcal{S}_{\mathrm{eff}} = -\operatorname{Tr}\left[\ln\left(\frac{-G^{-1}}{\hbar} \right) \right] - \int_0^{\hbar\beta} \mathrm{d}\tau \int \mathrm{d}\mathbf{x} \frac{|\Delta_{\mathbf{x},\tau}|^2}{g}, \tag{9}$$

where the inverse propagator can be written as the sum of an inverse 'free fermion propagator' and a term arising from the superfluidity:

$$-G^{-1} = -G_0^{-1} + F\,.$$

The inverse free fermion propagator is

$$-G_0^{-1} = \sigma_0 \left(\hbar \frac{\partial}{\partial \tau}\right) + \sigma_3 \left(-\frac{\hbar^2}{2m}\nabla_{\mathbf{x}}^2 - \mu\right)$$

and the superfluid part of the propagator can be written as

$$F = \sigma_0 \left(-\tfrac{1}{2}\,\mathbf{v}_{\mathbf{x},\tau}\cdot \mathrm{i}\hbar\nabla_{\mathbf{x}}\right) - \sigma_1 \left(\hbar\,|\Delta_{\mathbf{x},\tau}|\right) + \sigma_3 \left(\frac{\mathrm{i}\hbar}{2}\,\frac{\partial\theta_{\mathbf{x},\tau}}{\partial\tau} - \frac{\mathrm{i}\hbar}{4}\,\nabla_{\mathbf{x}}\cdot\mathbf{v}_{\mathbf{x},\tau} + \frac{m}{8}\,\mathbf{v}_{\mathbf{x},\tau}^2\right).$$

In these expressions, σ_0, ..., σ_3 are the Pauli matrices. Note that if we have an external potential $V_{\mathrm{ext}}(\mathbf{x})$ present, for example the optical potential or the magnetic trap, this appears in $-G_0^{-1}$ as an extra term $+\sigma_3 V_{\mathrm{ext}}(\mathbf{x})$. The effective action (9) depends on the fields $|\Delta_{\mathbf{x},\tau}|$, $\theta_{\mathbf{x},\tau}$. For these fields, a saddle point approximation is usually made. For example, a good saddle point form when no vortex is present is [15, 16]:

$$\begin{cases} |\Delta_{\mathbf{x},\tau}| = \Delta\,, \\ \theta_{\mathbf{x},\tau} = \text{constant}\,. \end{cases} \tag{10}$$

The value of the constant for the phase is irrelevant, and the value of Δ can be extracted by extremizing the effective action $\delta\mathcal{S}_{\mathrm{eff}}/\delta\Delta = 0$. This yields the well-known *gap equation* in the case of neutral atoms interacting through a contact potential. Alternatively, we proposed in Ref. [11] to use a different saddle point approximation to investigate the case of a fermionic superfluid containing a vortex parallel to the z-axis:

$$\begin{cases} |\Delta_{\mathbf{x},\tau}| = \Delta_r\,, \\ \theta_{\mathbf{x},\tau} = \phi\,. \end{cases} \tag{11}$$

Here, ϕ is the angle around the z-axis, and r is the distance to the z-axis. Again, a gap equation can be derived for Δ_r by extremizing the action — this gap equation yields a gap that depends on the distance to the vortex line (the z-axis). Fixing the total number of fermions yields a number equation in which the local density of fermions can be identified straightforwardly.

3 Results and discussion

Consider first the simplest saddle point approximation, (10). The saddle point result for the action in this case is

$$\mathcal{S}_{\mathrm{sp1}} = \frac{|\Delta|^2}{g} - 2\int \frac{\mathrm{d}\mathbf{k}}{(2\pi)^3} \ln\left[2\cosh\left(\frac{\beta}{2}\sqrt{\left(\frac{k^2}{2m}-\mu\right)^2 + |\Delta|^2}\right)\right].$$

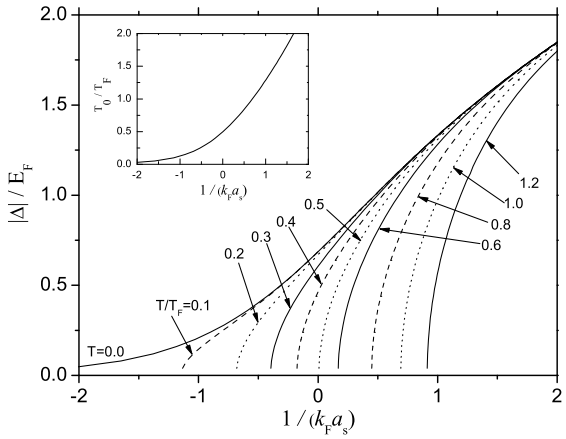

Fig. 2. The saddle point value Δ is shown as a function of the interaction strength parameter $1/(k_F a_s)$ for different values of the temperature. In the BCS regime this corresponds to the BCS gap and it vanishes at the critical temperature. The inset shows the temperature at which $\Delta = 0$. In the BEC regime, fluctuations around the saddle point need to be taken into account to obtain the correct critical temperature [15].

Two unknowns are the chemical potential μ and the value of constant Δ, the gap. The chemical potential is obtained by fixing the particle density. In the BCS limit, $\mu \to E_F$ whereas in the BEC limit, the chemical potential goes to the binding energy of the molecule, $\mu \to \hbar^2/(m a_s^2)$. In the intermediate regime, there is a smooth crossover between the two limiting values. The gap Δ is found by extremizing the saddle point action, $\delta \mathcal{S}_{\rm sp1}/\delta\Delta = 0$. The result is shown for different temperatures in figure 2. At temperature zero, the gap depends exponentially on the scattering length as we expect from the BCS theory. As the temperature is raised, the gap decreases, reaching zero at a certain temperature. In the BCS limit, the superfluidity is destroyed by breaking up Cooper pairs, so the critical temperature corresponds to the temperature where $\Delta = 0$. However, in the BEC limit, superfluidity is destroyed through phase fluctuations, and one cannot extract the critical temperature from the results shown in figure 2. It becomes necessary to include fluctuations around the saddle point value (10) and expand the effective action up to second order in these fluctuations around the saddle point value. This second-order expansion yields an action that is quadratic in the fluctuation variables and that can be integrated analytically. For fluctuations around the saddle point (10) this was done by Randeria and co-workers, who obtained a corrected value of the critical temperature that in the BEC limit becomes independent of $1/(k_F a_s)$.

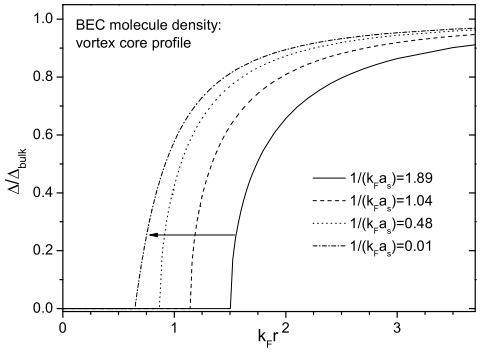

Fig. 3. The order parameter, as a function of the distance to the vortex core, for different values of the interaction parameter on the BEC side.

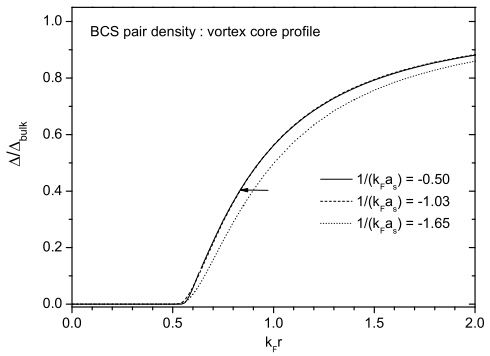

Fig. 4. The order parameter, as a function of the distance to the vortex core, for different values of the interaction parameter on the BEC side.

Next, we consider the saddle point approximation (11) suitable to describe a vortex. Extremizing the action leads to the following gap equation:

$$\frac{1}{k_F a_s} = \frac{2}{\pi}\int \mathrm{d}k \left(1 - \frac{k^2}{\sqrt{\left(k^2 - \mu + (k_F r)^{-2}/4\right)^2 + \Delta_r^2}}\right),$$

whereas the number equation becomes

$$\rho_r = \frac{3}{2}\int \mathrm{d}k\, k^2 \left(1 - \frac{k^2 - \mu}{\sqrt{\left(k^2 - \mu + (k_F r)^{-2}/4\right)^2 + \Delta_r^2}}\right).$$

Fixing the total number of particles $N = \int \mathrm{d}\mathbf{r}\, \rho_r$ allows to fix the chemical potential.

For a given chemical potential, solving the gap equation leads to a pair density $|\Delta_r|^2$ that depends on the distance r to the center of the vortex line.

The result is shown for different values of the interaction strength, in figures (3), (4). Starting with a vortex in a molecular condensate (deep in the BEC side), the vortex core will shrink as the interaction strength is increased. Crossing over the Feshbach resonance into the BCS side, the vortex core size R is seen to saturate at about $k_F R = \frac{1}{2}$. This is consistent with the idea that on the BEC side, the system can be well approximated by a collection of point bosons with twice the mass of the constituent atoms. In this molecular condensate, the healing length and thus the vortex core size will shrink as the interaction is increased. However, when one crosses into the BCS side, the fermionic pairs are no longer tightly bound molecules, but weakly bound, delocalized Cooper pairs, and the concept a the healing length based on point bosons is no longer valid.

4 Conclusion

In this contribution, we have first reviewed the path-integral description of the BEC/BCS crossover in dilute atomic gases. At low temperatures, the interatomic interaction can be appropriately modelled by a contact potential with renormalized strength, and this greatly simplifies calculations. We emphasize that the formalism is not restricted to a single choice of saddle point approximation. Indeed, by a judicious choice of the saddle point approximation to the Hubbard–Stratonovic fields, it is possible to investigate not only the ground state configuration, but also excited or metastable states. An example of this, worked out in this contribution, is the vortex state of the superfluid Fermi gas.

The Fonds voor Wetenschappelijk Onderzoek - Vlaanderen provides financial support for J.T. ('postdoctoraal mandaat'). This research has been supported financially by the FWO-V projects Nos. G.0435.03, G.0306.00, the W.O.G. project WO.025.99N, the GOA BOF UA 2000 UA, and the IUAP. J.T. gratefully acknowledges support of the Special Research Fund of the University of Antwerp, BOF NOI UA 2004.

References

[1] B. DeMarco and D.S. Jin: Science **285** (1999) 1703.

[2] B. DeMarco, S.B. Papp and D.S. Jin: Phys. Rev. Lett. **86** (2001) 5409.

[3] E. Tiesinga, B. J.Verhaar and H.T.C. Stoof: Phys. Rev. A **47** (1993) 4114.

[4] M.W. Zwierlein, C.A. Stan, C.H. Schunck, S.M.F. Raupach, S. Gupta, Z. Hadzibabic and W. Ketterle: Phys. Rev. Lett. **91** (2003) 250401.

[5] K.M. O'Hara, S.L. Hemmer, M.E. Gehm, S.R. Granade and J.E. Thomas: Science **298** (2002) 2179.

[6] C. Menotti, P. Pedri and S. Stringari: Phys. Rev. Lett. **89** (2002) 250402.

[7] C.A. Regal, M. Greiner and D.S. Jin: Phys. Rev. Lett. **92** (2004) 040403.

[8] M. Bartenstein, A. Altmeyer, S. Riedl, S. Jochim, C. Chin, J.H. Denschlag and R. Grimm: Phys. Rev. Lett. **92** (2004) 120401.

[9] M.W. Zwierlein, J.R. Abo-Shaeer, A. Schirotzek, C.H. Schunck and W. Ketterle: Nature **435** (2005) 1047.

[10] A. Bulgac, Y. Yu and J. Low: Temp. Phys. **138** (2005) 741.

[11] J. Tempere, M. Wouters and J.T. Devreese: Phys. Rev. A **71** (2005) 033631.

[12] M. Wouters, J. Tempere and J.T. Devreese: Phys. Rev. A **70** (2004) 013616.

[13] F.S. Cataliotti, S. Burger, C. Fort, P. Maddaloni, F. Minardi, A. Trombettoni, A. Smerzi and M. Inguscio: Science **293** (2001) 843.

[14] G. Orso, L.P. Pitaevskii and S. Stringari: Phys. Rev. Lett. **93** (2004) 020404.

[15] C.A.R. Sá de Melo, M. Randeria and J.R. Engelbrecht: Phys. Rev. Lett. **71** (1993) 3202.

[16] J.R. Engelbrecht, M. Randeria and C.A.R. Sá de Melo: Phys. Rev. B **55** (1997) 15153.

[17] S. De Palo, C. Castellani, C. Di Castro and B.K. Chakraverty: Phys. Rev. B **60** (1999) 564.

[18] H. Kleinert: Fortschr. Physik **26** (1978) 565.

[19] H. Kleinert: Annals of Physics **266** (1998) 135.

[20] A. Pelster: private communication.

[21] J.-P. Martikainen and H.T.C. Stoof: Phys. Rev. A **68** (2003) 013610.

[22] D.S. Petrov and G.V. Shlyapnikov: Phys. Rev. A **64** (2001) 012706.

[23] G. Orso, L.P. Pitaevskii, S. Stringari and M. Wouters: cond-mat/0503096.

[24] A. Smerzi, A. Trombettoni, P.G. Kevrekidis and A.R. Bishop: Phys. Rev. Lett. **89** (2002) 170402.

[25] F.S. Cataliotti, L. Fallani, F. Ferlaino, C. Fort, P. Maddaloni and M. Inguscio: New Journal of Physics **5** (2003) 71.